ARTICLE

ACS chemical biology

Structural Basis for Adenosylcobalamin Activation in AdoCbl-Dependent Ribonucleotide Reductases

Karl-Magnus Larsson[†,∥], Derek T. Logan[‡,*], and Pär Nordlund[†,§,*]

[†]Department of Biochemistry and Biophysics, Stockholm University, S-106 91 Stockholm, Sweden, [‡]Department of Biochemistry and Structural Biology, Lund University, Box 124, S-221 00 Lund, Sweden, and [§]Department of Medical Biochemistry and Biophysics, Karolinska Institute, S-171 77 Stockholm, Sweden. [∥]Present address: Department of Structural Biology, Stanford University School of Medicine, Stanford, California 94305-5126.

ABSTRACT Class II ribonucleotide reductases (RNR) catalyze the formation of an essential thiyl radical by homolytic cleavage of the Co–C bond in their adenosylcobalamin (AdoCbl) cofactor. Several mechanisms for the dramatic acceleration of Co–C bond cleavage in AdoCbl-dependent enzymes have been advanced, but no consensus yet exists. We present the structure of the class II RNR from *Thermotoga maritima* in three complexes: (i) with allosteric effector dTTP, substrate GDP, and AdoCbl; (ii) with dTTP and AdoCbl; (iii) with dTTP, GDP, and adenosine. Comparison of these structures gives the deepest structural insights so far into the mechanism of radical generation and transfer for AdoCbl-dependent RNR. AdoCbl binds to the active site pocket, shielding the substrate, transient 5′-deoxyadenosyl radical and nascent thiyl radical from solution. The e-propionamide side chain of AdoCbl forms hydrogen bonds directly to the α-phosphate group of the substrate. This interaction appears to cause a "locking-in" of the cofactor, and it is the first observation of a direct cofactor–substrate interaction in an AdoCbl-dependent enzyme. The structures support an ordered sequential reaction mechanism with release or relaxation of AdoCbl on each catalytic cycle. A conformational change of the AdoCbl adenosyl ribose is required to allow hydrogen transfer to the catalytic thiol group. Previously proposed mechanisms for radical transfer in B12-dependent enzymes cannot fully explain the transfer in class II RNR, suggesting that it may form a separate class that differs from the well-characterized eliminases and mutases.

Ribonucleotide reductases (RNRs) catalyze the transformation of ribonucleotides into deoxyribonucleotides, the precursors for DNA synthesis, by reduction of the C2′−OH bond. All RNRs use radical chemistry to catalyze this challenging reaction, and they can be divided into three major classes on the basis of their primary radical generation mechanisms (*1*–*3*). Despite diverse means of radical generation and storage, the three classes of RNR are unified by the subsequent channelling of the radical into a thiyl radical species in the structurally conserved active site (*4*). Class II RNR is different from the other two classes, as no accessory proteins are required for its radical generation. Instead, a transient 5′-deoxyadenosyl radical is generated by the homolytic cleavage of the Co–C bond between the Ado axial ligand and the Co(III) species of coenzyme B12 (adenosylcobalamin, AdoCbl) (*5*). This radical in turn generates a transient thiyl radical on an active site cysteine residue (*4*). The class II RNR is a member of a wider family of B12-dependent enzymes catalyzing radical substrate rearrangement reactions (*6*). This occurs through the direct interaction of the 5′-dAdo radical with the substrates, with the single exception of RNR, in which the radical is transferred *via* the aforementioned cysteine (*6*). These enzymes can be divided into three classes based on the reactions catalyzed and on the nature of the electroparamagnetic resonance spectra of their biradicals: class I mutases, class II eliminases, and class III aminomutases (*6*, *7*). The B12-dependent RNR has previously been classified as an eliminase (*7*).

The homolysis reactions catalyzed by B12-dependent enzymes are remarkable, as the rate of Co–C bond ho-

*Corresponding authors, derek.logan@mbfys.lu.se, par.nordlund@ki.se.

Received for review April 1, 2010 and accepted July 30, 2010.

Published online July 30, 2010

10.1021/cb1000845

molysis is increased by a factor of 10^9-10^{14} compared to that in solution. Kinetic, structural, and theoretical studies of B12 enzymes catalyzing a broad range of radical-dependent reactions have led to several different proposals for the mechanistic background to this rate enhancement (*8*–*11*). Concerted scenarios where Co–C bond homolysis is coupled to substrate oxidation or protein radical formation have been outlined, as well as stepwise mechanisms. Several lines of evidence point to control of the B12 binding mode as the key step in activation of the Co–C bond. For diol dehydratase substrate binding has been proposed to induce conformational strain in the cofactor, which would weaken the Co–C bond (*12*). On the basis of a modeling study, a rotation of the ribose unit about the glycosidic bond was then proposed to span the distance between the substrate and 5′-C radical immediately after bond homolysis (*13*). This mechanism has recently been shown to be plausible for the structurally related enzyme ethanolamine ammonia lyase (*14*). A similar but subtly different mechanism has been proposed for glutamate mutase, in which ribose *pseudorotation* (exchange between C2′-endo and C3′-endo puckers) mediates the necessary translation of the C5′ radical (*15*). Both of these conformations were experimentally observed in a high-resolution crystal structure. Theoretical studies using different computational strategies have led to the common conclusion that the protein interactions with the ribose group make major catalytic contributions to adenosylcobalamin activation, although the extent to which these effects are dominated by electrostatics or strain still remains a subject of discussion (*10, 11*).

Kinetic studies on class II RNRs to date have been dominated by the monomeric enzyme from *Lactobacillus leichmannii* (llNrdJ, also referred to as RTPR). Bond homolysis in this system has been studied in detail using two different substrate-free model reactions. *L. leichmannii* NrdJ can catalyze exchange of ^{3}H from the C5′ atom of AdoCbl, indicative of homolysis-related hydrogen transfer. This reaction is completely dependent upon the presence of the thiyl radical cysteine (Cys408 in llNrdJ) (*16*), which initially suggested a concerted reaction mechanism in which the Co–C bond breakage is made kinetically feasible through coupling to a hydrogen atom transfer step. Hydrogen exchange is also dependent on the presence of specificity effectors, where dGTP is significantly more active than other effectors in enhancing the reaction rate. An unusually high entropy of activation for the hydrogen exchange reaction and a large hydrogen isotope effect were also observed (*17*), although other studies came to the contrasting conclusion that the reaction was almost entirely enthalpically driven (*18*). Later experiments, however, called into question the idea of a concerted mechanism. *L. leichmannii* NrdJ can also catalyze epimerization of the adenosyl C5′ hydrogen atoms under similar reaction conditions (*19, 20*) to those favoring 5′-H exchange (*19*). However epimerization, in contrast to hydrogen exchange with solvent, is not dependent on the presence of Cys408. This suggested the feasibility of a stepwise mechanism where the initiation of Co–C bond breakage is primarily mediated by events related to the cofactor binding mode. At present the stepwise mechanism seems to be the most plausible scenario for B12-dependent RNR.

The crystal structure of the monomeric *L. leichmannii* class II RNR in complex with the AdoCbl analogue adeninylpentylcobalamin (AdePeCbl) has been determined (*20*). A B12-binding domain was identified consisting of an insertion between strands βH and βI of the conserved 10-stranded α–β barrel of RNRs, as well as part of the sequence C-terminal to the barrel, following strand βJ. Although this crystal structure allowed the positioning of the corrin ring and the dimethylbenzimidazole (DMB) axial ligand of Co, no model for the adeninylpentyl moiety was presented. A hinge-like closure of the B12-binding domain was noted, which could reflect switching between open and closed forms of the enzyme upon cofactor binding. It was concluded that the structure of llNrdJ with AdePeCbl corresponds to a partially opened conformation, as the distance between the cobalt ion and the thiyl radical site was around 10 Å, as compared to the 5.5–7.5 Å expected from EPR measurements (*21*). Thus the mechanisms of Co–C bond homolysis and radical transfer in class II RNR remain unclear, and further structural investigations are clearly required.

RESULTS AND DISCUSSION

The tmNrdJ protein construct used in the present study lacks the 82 C-terminal residues, which contain cysteine residues essential for enzyme regeneration using the physiological reduction system. However this truncated enzyme is fully active in the presence of dithiothreitol (DTT), as described previously (*22, 23*). The crystal struc-

ture of tmNrdJ in complex with dTTP, GDP, and AdoCbl has been solved at a resolution of 1.9 Å, while the dTTP/GDP/Ado and dTTP/AdoCbl complexes have both been determined to 1.8 and 1.95 Å, respectively.

dTTP/GDP/AdoCbl Complex. The dTTP/GDP/AdoCbl complex provides several essential details of cofactor binding and illuminates the mechanism of Co–C bond cleavage. The electron density for AdoCbl is better defined in one monomer (chain B) than in the other, presumably due to crystal packing effects that cause a slightly different conformation of the B12-binding domain in chain A that reduces its interactions with AdoCbl. This phenomenon is also evident in the dTTP/AdoCbl complex. Nevertheless the electron density for AdoCbl is very good in chain B (Figure 1, panel a). AdoCbl binds to the surface of tmNrdJ, and its 5,6-dimethylbenzimidazole (DMB) moiety is relatively exposed. However, it cannot be excluded that interactions from the 82 C-terminal residues absent in this construct further close off the active site in the full-length enzyme, as the C-terminus of the truncated tmNrdJ is exactly in this region. The corrin ring is positioned between the C-terminal tips of strands I and J of the RNR α/β barrel on its AB (or "north") side and loop 2, the catalytic Cys322-containing finger loop and the substrate GDP on the CD (or "south") side (Figure 1, panels a and b). Two methyl groups of the corrin make van der Waals (vdW) interactions to Phe508 and Tyr628, while the linker to the DMB moiety protrudes into a pocket formed by the N-terminal helix (residues 17–26) and the B12 binding motif identified in llNrdJ (*20*), which consists of an insert following the helix that binds the substrate α-phosphate (residues 499–577), as well as the C-terminal residues (633–726). The corrin side chains anchor it to Asp295 on strand βD, Asn600 on βI, and Asp630 just after βJ, either directly or through water molecules (Figure 1, panel b). Most interestingly the e-propionamide side chain of AdoCbl makes direct H-bonds to the α-phosphate of the substrate GDP, effectively burying the latter from direct solvent access. Less extensive interactions are made with the B12 binding motif. This could be due to the lack of some C-terminal structure in the truncated variant, *i.e.*, the third strand of the B12 binding domain and two helices that buttress the back of this domain in llNrdJ.

AdoCbl in tmNrdJ is bound in a more closed conformation of the enzyme compared to llNrdJ (Figure 2). The cobalt–thiol radical site distance is 7.3 Å in tmNrdJ, as compared to 10 Å in llNrdJ, and the cofactor in tmNrdJ makes more extensive interactions with the residues of the α/β barrel. The Co–Cys distance in tmNrdJ corresponds well to the range of 5.5–7.5 Å determined by EPR spectroscopy for llNrdJ (*4*), suggesting that the tmNrdJ structure shows the cofactor at its final position prior to bond homolysis.

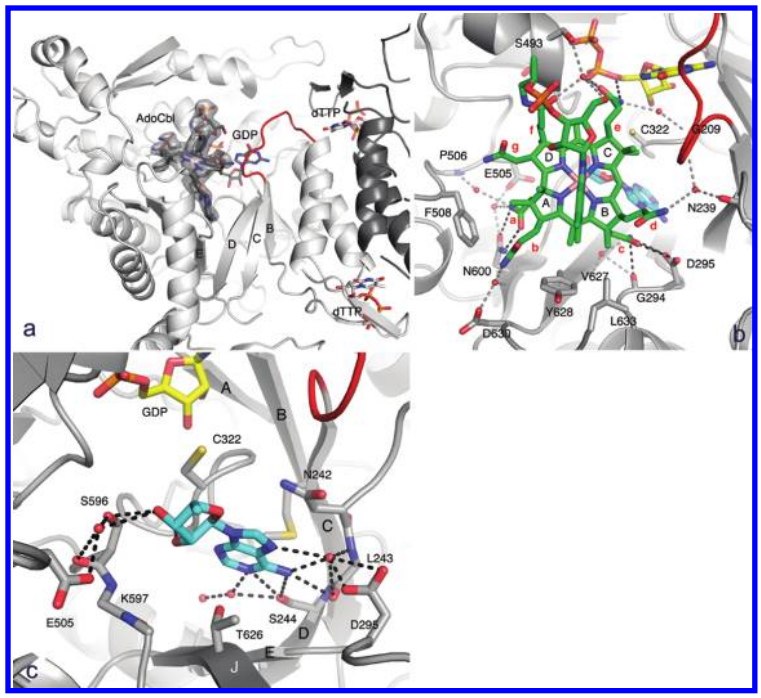

Figure 1. Structural interactions of the tmNrdJ enzyme with dTTP, GDP, and AdoCbl. a) Overall view of the active site of tmNrdJ in complex with dTTP, GDP, and adenosylcobalamin tmNrdJ is shown as a cartoon. Monomer B is colored in light gray, and monomer A is dark gray. β-Strands in the first half of the α/β barrel are labeled with capital letters. Allosteric effector dTTP, substrate GDP (yellow), and cofactor AdoCbl are shown as sticks. Electron density for AdoCbl is shown as a transparent gray surface. The map has coefficients $2m|F_o| - D|F_c|$ and is contoured at 1.0 σ. b) Details of the interaction of the corrin ring with tmNrdJ. Monomer B of tmNrdJ is shown as a gray cartoon. Otherwise the color scheme is as in panel a. Residues making polar or van der Waals' contact with the corrin moiety are shown as sticks. Hydrogen bonds to corrin are shown as dotted lines. c) Interactions of the adenosyl moiety of AdoCbl with its binding pocket. The adenosyl group is shown as a stick model (cyan) with corrin moiety of AdoCbl removed for clarity.

Binding of the Deoxyadenosyl Moiety. The 5′-deoxyadenosyl (5′-dAdo) base of AdoCbl points into a well-defined binding pocket at the top of the α/β barrel between β-strands D and E (Figure 1, panels a and c). The base is sandwiched between Asn242 at the beginning of βD and Thr626 on βJ (Figure 1, panel c). Asn242 is locked in place by an H-bond to the carbonyl oxygen

Figure 2. Comparison of the AdoCbl cofactor position in the monomeric NrdJ from *L. leichmannii* (llNrdJ) and the dimeric NrdJ from *T. maritima* (tmNrdJ). Superpositioned structures of the two enzymes llNrdJ (orange) complexed with AdePeCbl (light orange stick model) and one monomer of tmNrdJ plus the dimerization helices of the other monomer, with AdoCbl (dark gray stick model). The tmNrdJ enzyme forms a more closed complex with AdoCbl, which results in a catalytically feasible distance to the radical cysteine in the active site, shown with substrate GDP (from the tmNrdJ structure, dark gray). Several secondary structure elements and the second monomer of tmNrdJ have been removed for clarity.

of Pro321 in the finger loop, immediately preceding the radical cysteine Cys322 (which corresponds to Cys408 in llNrdJ). The base is in the *anti* conformation relative to the ribose and makes several polar interactions, directly or through bound water molecules, to residues of the binding pocket, which are conserved or conservatively substituted in the sequences of more than 200 class II RNRs retrieved from the RNRdb (*24*). The Ado C5′ atom is 6.5 Å from the Sγ atom of Cys322, to which the radical should be transferred.

The electron density does not permit us to identify unambiguously the ribose pucker, but it is significantly closer to C2′-endo than C3′-endo. Co-refinement of both C2′-endo and C3′-endo puckered ribose does not significantly improve the fit to the density. The Co−C5′ distance is 2.7 Å, which is significantly longer than expected for an unbroken Co(III)−C bond (2.0 Å) but shorter than for a fully broken Co(II)–C bond (3.0 Å). It is therefore possible that the structure corresponds to a mixture of two or more states with one of them predominating or several states with very similar structures.

Apart from small changes in the B12-binding domain, the presence of the cofactor does not induce any large conformational changes of the overall tmNrdJ structure compared to the dTTP/GDP complex (*25*). Thus one can regard the β-barrel domain of tmNrdJ as a relatively rigid framework to bind and modulate the geometry of AdoCbl. However the loop 2 conformation in this complex is somewhat ambiguous: it clearly does not have the same conformation as in the complex without AdoCbl (*25*), but the electron density is weak and loop 2 may exist in a mixture of conformations linked to the presence of some GDP bound to the active site in an artifactual "backwards" orientation (see Supplementary Figure 1).

dTTP/AdoCbl Complex. This complex represents the situation in which the cofactor has bound to the enzyme in the absence of substrate. Electron density for the corrin ring, DMB moiety, and linker is poorer than in the complex including substrate, indicating lower occupancy or higher mobility. Though clearly present, electron density for the 5′-dAdo moiety is also poorer than in the quaternary complex including substrate. Nevertheless the corrin side chains clearly define the orientation of the ring. Strikingly, the cofactor is not bound in the same orientation as in the dTTP/GDP/AdoCbl complex (Figure 3). The corrin ring is rotated by 11° around a pivot point at the b-propionamide group on the substrate-distal side of the ring. This results in a 0.7 Å translation of the Co atom relative to the complex with substrate. The rotation toward the orientation seen in dTTP/GDP/AdoCbl is clearly made possible by the interaction of the e-propionamide side chain with the α-phosphate group of the substrate. Loop 2 is disordered in this complex, as expected in the absence of GDP from our earlier work (*25*). Since the cofactor in the dTTP/AdoCbl complex also blocks substrate access to its binding pocket, this form cannot be considered part of a plausible enzymatic reaction cycle, but it is relevant for understanding previous biochemical studies of epimerization (see below).

Adenosine Complex. We soaked crystals of tmNrdJ with free adenosine in order to examine the behavior of this part of the cofactor in the absence of stereochemical constraints from the corrin ring. Two different binding modes are observed in the two monomers of the crystallographic asymmetric unit (Figure 4). The adenine base in both monomers occupies the same pocket as in the dTTP/GDP/AdoCbl complex, but only the adenine

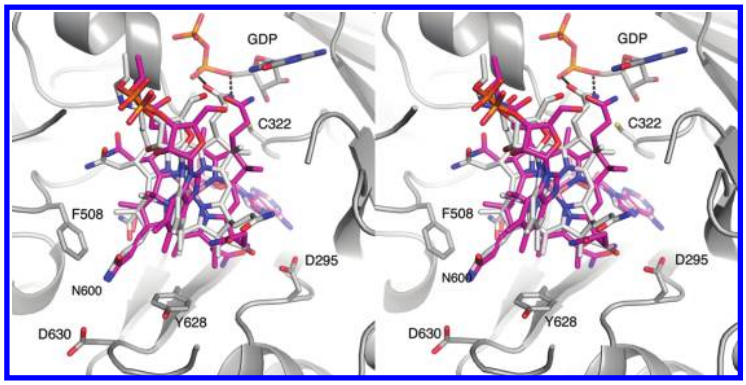

Figure 3. Comparison of the positions of the corrin ring in AdoCbl complexes in the presence and absence of substrate. Stereoview of superpositioned structures of the dTTP/AdoCbl complex (magenta) and the dTTP/GDP/AdoCbl complex (gray). In the substrate-containing complex the corrin ring is rotated 11° relative to the dTTP/AdoCbl complex. It forms two hydrogen bonds to GDP, which illustrates a possible final reorientation of the ring, locking in the active site.

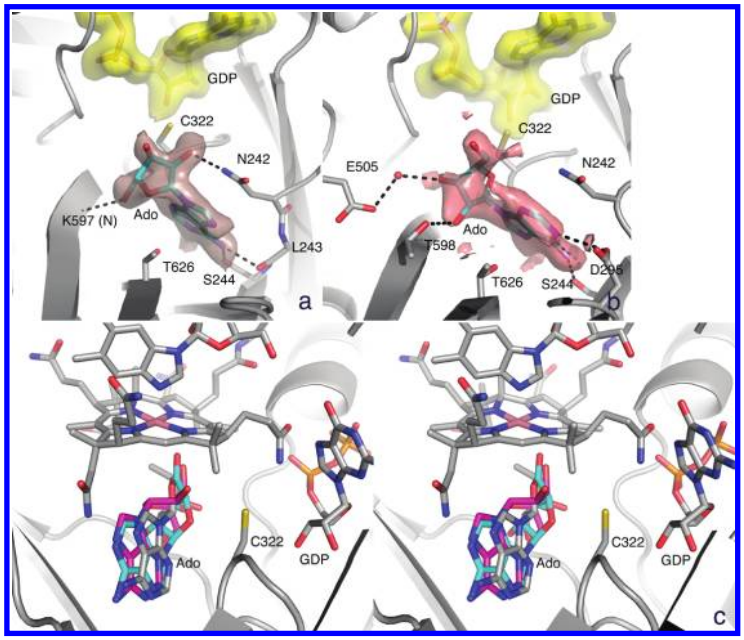

Figure 4. Details of the two adenosine conformations observed in the dTTP/GDP/Ado complex. a) Conformation in monomer A. b) Conformation in monomer B of the two crystallographically independent monomers in the asymmetric unit. Hydrogen bonds from adenosine are shown as dotted lines. The electron density is an $m|F_o| - D|F_c|$ map with phases obtained after omitting GDP and adenosine from the model, contoured at 3.0 σ for GDP (yellow) and 2.5 σ for adenosine (red). c) Stereoview comparing the two adenosine conformations A (magenta) and B (cyan) with the one observed in the dTTP/GDP/AdoCbl complex (gray).

in the A-subunit has the same orientation as in the presence of the corrin ring. Nevertheless the ribose groups are positioned in the same region in both complexes. In the conformation seen in subunit B (Figure 4, panel a) C5′ is further from the Co atom than in the superimposed AdoCbl complex (3.5 *vs* 3.0 Å) and closer to Cys322 (4.4 *vs* 6.5 Å). In subunit A the 5′ carbon atom is projected into the interior of the protein (Figure 4, panel b). The 5′-OH group is of course absent in the 5′-dAdo moiety of the true cofactor. Interestingly, in both adenosine conformations, and in contrast to the AdoCbl complex, the base is *syn* with respect to the ribose, which has a C2′-endo pucker. The structures of the adenosine complexes suggest that the adenine pocket is largely predefined for binding the base but that, expectedly, more versatile interaction modes with the ribose are possible in the absence of restraints from the corrin ring.

The three complexes of tmNrdJ presented here provide for the first time a detailed view of the machinery for radical generation in a ribonucleotide reductase. The binding site of AdoCbl both in the presence and absence of substrate corresponds to a closed form of the enzyme as regards the B12-binding domain, and the 5′-dAdo binding pocket can be clearly delineated. The model for the 5′-Ado moiety in the dTTP/GDP/AdoCbl complex reflects a conformation close to the Co–C bond cleavage stage. The Co–thiyl radical site distance observed is consistent with measurements made by EPR for the llNrdJ enzyme (*4*), indicating that the states observed here for a dimeric

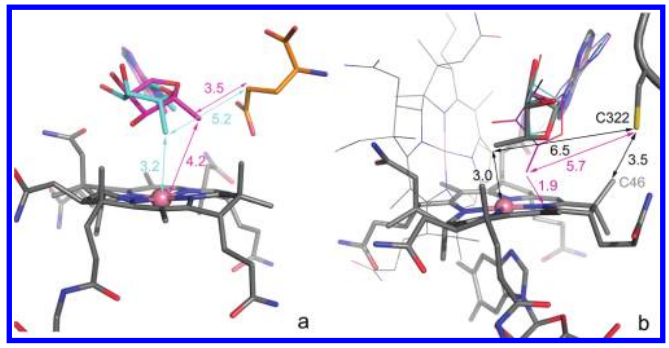

Figure 5. Comparions of radical transfer geometry in glutamate mutase and ribonucleotide reductase. a) The ribose pseudorotation model proposed for glutamate mutase (GM). A pseudorotation of the adenosyl ribose from C2′-endo (cyan) to C3′-endo (magenta) in GM transports the C5′ adenosyl radical from 5.2 Å to within 3.5 Å of the Cγ atom of the substrate, from which it can then abstract a hydrogen atom. b) A ribose pseudorotation cannot adequately explain radical transfer in tmNrdJ. The orientation of this panel is rotated approximately 90° clockwise with respect to panel a. The corrin ring of GM is shown in thin gray lines to illustrate its very different relationship to the adenosine moiety in the two enzymes. The C2′-endo conformation of the Ado moiety in glutamate mutase (thin purple lines) has been superimposed on its equivalent in tmNrdJ (gray sticks). Pseudorotation to the C3′-endo form (thin magenta lines) would bring C5′ to only 2.1 Å from Co, while also bringing C5′ into van der Waals' contact with atoms on the substrate-proximal side of the corrin ring. Thus some relaxation of the cofactor is apparently required for radical transfer. Note that in this conformation C46 of the corrin ring is in vdW contact with the Sγ atom of Cys322.

class II RNR are also directly relevant for the less common monomeric enzymes. Cobalamin also forms a lid over the part of the active site involved in radical chemistry, thereby shielding these reactions from radical scavengers, as in other B12-dependent enzymes. Moreover, the burial of the substrate implies an ordered sequential reaction mechanism in which AdoCbl is released or at least relaxed from this position in each reaction cycle in order to allow product release and new substrate binding. This may be accomplished by a hinge movement of the B12-binding domain toward a state more similar to the llNrdJ complex (*20*).

The activation of the Co–C bond in AdoCbl-dependent enzymes has generated great interest and a number of different mechanistic proposals. Theoretical and chemical studies have now largely dismissed the DMB ligand as a major determinant in modulation of Co–C bond strength (*26, 27*). In some AdoCbl-dependent enzymes a direct coupling of substrate radical generation to Co–C bond homolysis as been suggested to be important for activation (*8, 16*). Theoretical studies of mutases have indicated that the trapping of the Ado C5′ radical in the close vicinity of the corrin ring is energetically favorable (*10*). Steric and electrostatic effects on the Ado ribose moiety have also been suggested as key factors in catalysis, although the nature of these effects remains controversial (*10, 11*).

In the tmNrdJ structures two well-defined binding sites for the corrin and 5′-Ado moieties of AdoCbl have been identified. A notable feature is the rigid binding pocket for AdoCbl, which provides a well-defined matrix for polar and vdW interactions essential for binding and promotion of homolysis. The binding pocket contains the C5′ radical within the close environment of the Co(II) ion. The pocket is also well constituted for controlling the environment of the ribose group during catalysis. The notion that the bond homolysis is likely to be reversible, *i.e.*, that the cofactor is regenerated in each cycle (*28*), is consistent with the hypothesis that no major conformational changes are made in this region of the protein during the reaction.

The binding of substrate locks the corrin ring in its final position through a direct interaction between the e-propionamide side chain and the α-phosphate group common to all ribonucleotide substrates, which could affect the accessible conformational space for the 5′-Ado group and thereby the catalytic rate. However, it has been demonstrated that an epimerization reaction, indicative of Co–C bond homolysis, is also catalyzed by the substrate-free llNrdJ enzyme when an allosteric effector is present (*19*). Thus generation of the adenosyl radical does not necessarily need to be coupled to the subsequent generation of a cysteinyl radical, *i.e.*, it could be a stepwise reaction. The complex of tmNrdJ with AdoCbl in the absence of substrate might be directly relevant to the epimerization reaction in llNrdJ. Without substrate AdoCbl can bind to tmNrdJ, but not in its final conformation, as a rotation of 11° is induced by H-bonds to the α-phosphate of the substrate. Interestingly the K_D value for binding of AdoCbl to C408S-llNrdJ is 132 ± 10 μM (*19*) and the K_M in a ^{3}H washout reaction in the absence of substrate is 60 ± 9 μM (*16*), whereas K_M in the true reduction pro-

cess is 0.25 μM, indicating a 10^2- to 10^3-fold increase in affinity when substrate is present (*16*). Our structures explain this increase by implicating the substrate directly in correct binding of the cofactor. However, the exact role of the 11° rotation for Co–C bond activation remains uncertain, as both forms catalyze Co–C bond cleavage. The quality of electron density for the 5′-dAdo moiety in the dTTP/AdoCbl complex unfortunately does not allow a definitive determination to what extent further strain is imposed upon the Co–C bond by this rotation.

By analogy with the mutases, the enzyme interactions with the 5′-Ado ribose are also likely to be important for class II RNR Co–C bond homolysis. Some investigators have advocated that the bond activation is primarily electrostatic in nature and achieved through stabilization of the transition state rather than destabilization of the reactant state (*11*). On the other hand the Co–C bond cleavage in almost all AdoCbl-dependent enzymes has been described as a simple bond dissociation process with no well-defined transition state (*6, 7*). As no significant charge separation occurs during Co–C bond breakage, electrostatic stabilization is suggested to be effected through the polar ribose moiety. In the mutases, charged groups, primarily carboxylates, are thought to promote this catalytic effect through interactions with the ribose (*11*). Polar effects on the ribose in tmNrdJ might be imposed by hydrogen bonds with neutral polar residues, but no direct interactions are made by charged groups. However the highly conserved Glu505 is found on one face of the ribose binding pocket and could potentially play a role in catalysis by water-mediated interactions with the ribose or alternatively by making direct interactions in a different conformation of the ribose or Glu505 side chain.

How is the radical transferred to Cys322? The relative proximity of the 5′-carbon atom to Cys322 in our structure (6 Å) supports the idea that a direct hydrogen atom transfer between C5′ and Cys322 might be possible after Co–C bond cleavage. However the distance in our present model is too long for a direct H-transfer, and a conformational change is required. Together the AdoCbl and the Ado complexes imply that, while the adenine base is rigidly bound, the ribose moiety has more freedom to change conformation. This situation is similar to that of the mutases, where a conformational change is required for radical transfer, to allow C5′ to be positioned for direct hydrogen atom transfer from the substrate. Two different but related mechanisms for radical transfer have been proposed, namely, ribose *rotation* around the glycosidic bond for the base-on enzyme diol dehydratase (*8*) and ribose *pseudorotation* for the base-off enzyme glutamate mutase (*15*). From our present structures we cannot conclude directly which if either of these mechanisms is operative in class II RNR. Nevertheless a superposition of the cofactors of tmNrdJ and glutamate mutase (GM) affords valuable insights. The 5′-dAdo binding mode is very different in GM (Figure 5, panel a), with the base almost parallel to the corrin ring (*15*). In contrast, the 5′-dAdo moiety of AdoCbl in tmNrdJ superimposes very well with that of the "intact" conformation in GM, which also has the C2′-endo pucker. The ribose pseudorotation model postulates a conformational exchange between this conformation and a C3′-endo "broken" state in which C5′ moves to within 3.5 Å of the radical destination, the substrate C_β atom (*15*). However the direction of movement of the radical in GM is perpendicular to the corrin, while in tmNrdJ it is parallel to it. A similar pseudorotation from C2′-endo to C3′-endo in tmNrdJ would actually move C5′ closer to Co, to approximately 2.0 Å, and would still leave it 5.7 Å from Cys322 (Figure 5, panel b).

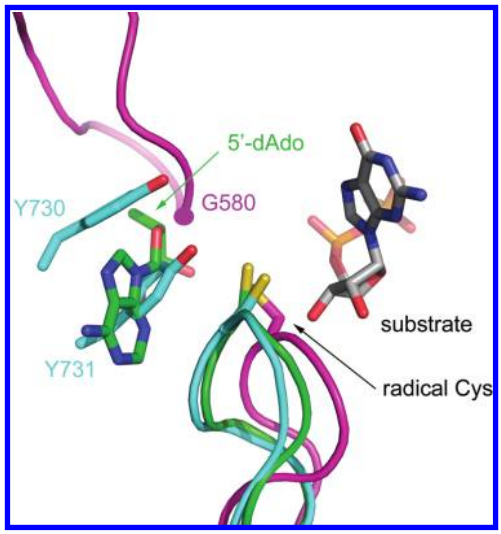

Figure 6. Congruence of the radical transfer pathway end points in all three classes of RNR. The *E. coli* class I (cyan), *T. maritima* class II (green), and bacteriophage T4 class III (magenta). The RNR structures are shown in highly simplified form, with only the finger loop, radical cysteine, and end points of the radical generation or transfer pathway drawn.

Thus pure rotation around the glycosidic bond, or a combination of rotation and pseudorotation, seems more likely for NrdJ. However, along the path traversed by C5′ during a simple rotation around the glycosidic bond from our AdoCbl conformation to a productive hydrogen transfer position, it would come into vdW contact with atoms in the D ring of the corrin backbone, especially C11 and one of the methyl groups on C12 (C46; see the Supplementary Movie). Therefore the rotation is likely to require additional conformational changes, most likely a relaxation of the corrin ring.

Interestingly, allosteric substrate specificity effectors, in particular dGTP, have been shown to be necessary for homolysis of the Co–C bond in all experiments involving the *L. leichmanii* enzyme. This suggests a role for the effectors in fine-tuning the B12 binding mode. Our recent detailed model for allosteric regulation in class II RNRs (*25*) identified the role of the effectors in modulating an ensemble of conformations of loop 2. Although loop 2 approaches the cofactor quite closely (Figure 1, panels a and b), no unambiguous interactions can be observed, and the disorder in loop 2 in the AdoCbl complexes precludes a more detailed analysis at the present time.

Convergent Evolution of Chemically Diverse Radical Transfer Pathways in RNR. The complexes presented here confirm and further illuminate the striking congruency of the end points of the radical generation and/or transfer pathways in all three classes of RNR (Figure 6), first suggested on the basis of the position of the corrin ring and Co atom in the llNrdJ/AdePeCbl structure (*19*). In class I RNR the a tyrosine radical is generated on a separate subunit and transferred through a hydrogen-bonded pathway to the radical cysteine (*1*). The distance from the hydroxyl group of the last tyrosine residue (Tyr731) in the radical transfer chain to Sγ of Cys439 in class I RNR is 3.4 Å (*29*). In class III RNRs a radical is generated on the Cα atom of a Gly residue in a C-terminal loop close to the radical cysteine. The distance between this atom and Sγ of Cys290 in an oxygen-stable Gly → Ala mutant of the class III RNR from bacteriophage T4 is 5.5 Å (*30*). The distance from the transient radical on C5′ to Cys322 in class II is 6.5 Å immediately after bond homolysis, and possibly 4.4 Å after relaxation of the cofactor (this work). The convergent evolution of radical transfer pathways in the three classes of RNR was already hinted at in the "open" form represented by llNrdJ (*20*), but the present dTTP/GDP/AdoCbl complex, by localizing the 5′-deoxyadenosyl moiety of the cofactor, further underlines the structural basis for the recruitment of diverse radical generation mechanisms to a common framework for radical utilization in the RNR family.

METHODS

Purification and Crystallization. The *T. maritima* class II ribonucleotide reductase tmNrdJ was produced and crystals were grown using a C-terminally truncated construct (residues 1–644) as described previously (*25*). Soaking experiments were carried out using times and concentration of nucleotides and cofactors as indicated in Table 1 and Supplementary Table 1. Crystals were flash frozen in liquid nitrogen in a 1× concentrated cryo solution consisting of 8–12% PEG (w/v) PEG 8000, 0.1 M Na acetate buffer pH 4.5, 0.1 M NaCl, 20% (v/v) glycerol. Nucleotides, $MgCl_2$, DTT and water were added to a 1.6× cryo solution to obtain the final 1× solution. Both adenosylcobalamin and adenosine were dissolved in the 1.6× buffer to obtain final concentrations in 1× buffer as indicated in Table 1. The soaking experiments were performed at RT (~20 °C), and all manipulations involving adenosylcobalamin, up to and including freezing of crystals, were performed under dim red light.

Data Collection and Processing. Data collection was performed under ambient light at 100 K using beamlines ID14-3 and ID29 of the ESRF, Grenoble, France and I711 and I911-5 of MAX-lab, Lund, Sweden. The data were processed and scaled with XDS (*31, 32*). Crystals of all three complexes belong to space group *C*2 with one tmNrdJ dimer in the asymmetric unit. Data statistics are listed in Table 1. The CCP4 suite was used for all crystallographic data manipulations (*33, 34*).

Structure Determination and Refinement. The different complexes were isomorphous and new structures were determined using high-resolution tmNrdJ structures (*25*) as starting models in refinement using Refmac5, without recourse to molecular replacement. In the latter stages phenix.refine with TLS refinement was used (*35*). For both programs a restraints file was generated using a recent high-resolution crystal structure of AdoCbl (*36*). Manual model building was performed in O (*37*) and Coot (*38*). Arp_waters (CCP4 suite) was used for water addition. Structures were superimposed using the SSM algorithm (*39*) in Coot. Cofactors were superimposed using the pair-matching wizard in Pymol (www.pymol.org). All figures were made using Pymol.

Accession Codes: The structures have been deposited in the Protein Data Bank with accession codes 3O0O for dTTP/GDP/AdoCbl, 3O0N for dTTP/AdoCbl, and 3O0Q for dTTP/GDP/Ado.

Acknowledgment: We wish to thank the staff at MAX-lab and the ESRF for technical help with data collection and Fahmi Himo for discussion. We thank Catherine Drennan for the kind gift of the llNrdJ coordinates in complex with adeninylpentylcobalamin. This work was supported by grants from the Swedish

TABLE 1. Data collection, processing, and model refinement statistics

	dTTP/AdoCbl	dTTP/GDP/AdoCbl	dTTP/GDP/Ado
Effector (mM)	0.4	0.4	0.4
Substrate (mM)	n/a	2	2
Cofactor (mM)	~25	~25	50
$MgCl_2$ (mM)	8	8	8
Soak time (h)	3	3	3
Beamline	ID14-3	ID29	I911-5
Resolution[b]	20–1.95 (2.00–1.95)	49–1.90 (2.00–1.90)	25–1.80 (1.90–1.80)
Unit cell dimensions			
a, *b*, *c* (Å)	119, 124, 107	120, 124, 107	119, 124, 107
β (deg)	103.1	102.6	103.4
Completeness (%)	99.1 (99.7)	99.4 (99.6)	99.0 (99.9)
Observed reflections	480845	530391	434380
Unique reflections	108084	119789	138738
$\langle I/\sigma(I)\rangle$	10.2 (1.59)	12.09 (1.60)	8.91 (2.24)
Wilson B-factor (Å^2)	30.5	31.5	22.4
R_{merge} (*I*)	8.3 (80.5)	6.4 (84.8)	7.5 (47.4)
R_{model} (*F*)	20.3 (38.5)[c]	20.2 (40.7)[d]	17.6 (28.4)[e]
R_{free} (*F*)	24.9 (40.7)[c]	23.8 (42.6)[d]	21.0 (32.3)[e]
Non-hydrogen atoms	10466	10787	11000
Water molecules	513	463	905
rms deviations from ideal geometry[f]			
Bond length (Å)	0.007	0.008	0.007
Bond angles (deg)	1.08	1.14	1.09
PDB codes	3O0N	3O0O	3O0Q

[a] $R_{merge}(I) = \Sigma_{j,k}|I_{jk} - \langle I\rangle_j|/\Sigma_{j,k}I_{jk}$, where I_{jk} are the *k* individual observations of each reflection *j* and $\langle I\rangle_j$ is the value after weighted averaging. $R_{model}(F) = \Sigma_h||F_o(h)| - |F_c(h)||/\Sigma_h|F_o(h)|$, where $|F_o(h)|$ and $|F_c(h)|$ are the amplitudes of the observed and calculated structure factors for reflection *h*. [b] Values in parentheses correspond to the highest resolution shell in data processing. [c] 1.97–1.95 Å. [d] 2.02–1.95 Å. [e] 1.97–1.90 Å; highest resolution shells in refinement (*35*). [f] As calculated using Molprobity (*40*).

Research Council to D.T.L. and P.N. and the Swedish Cancer Society to P.N.

Supporting Information Available: This material is available free of charge *via* the Internet at http://pubs.acs.org.

REFERENCES

1. Jordan, A., and Reichard, P. (1998) Ribonucleotide reductases, *Annu. Rev. Biochem. 67*, 71–98.
2. Nordlund, P., and Reichard, P. (2006) Ribonucleotide reductases, *Annu. Rev. Biochem. 75*, 681–706.
3. Eklund, H., Uhlin, U., Färnegårdh, M., Logan, D. T., and Nordlund, P. (2001) Structure and function of the radical enzyme ribonucleotide reductase, *Prog. Biophys. Mol. Biol. 77*, 177–268.
4. Licht, S., Gerfen, G. J., and Stubbe, J. (1996) Thiyl radicals in ribonucleotide reductases, *Science 271*, 477–481.
5. Tamao, Y., and Blakley, R. L. (1973) Direct spectrophotometric observation of an intermediate formed from deoxyadenosylcobalamin in ribonucleotide reduction, *Biochemistry 12*, 24–34.
6. Brown, K. L. (2005) Chemistry and enzymology of vitamin B12, *Chem. Rev. 105*, 2075–2149.
7. Brown, K. L. (2006) The enzymatic activation of coenzyme B12, *Dalton Trans.* 1123–1133.
8. Toraya, T. (2003) Radical catalysis in coenzyme B12-dependent isomerization (eliminating) reactions, *Chem. Rev. 103*, 2095–2127.
9. Banerjee, R., and Ragsdale, S. W. (2003) The many faces of vitamin B12: catalysis by cobalamin-dependent enzymes, *Annu. Rev. Biochem. 72*, 209–247.
10. Jensen, K. P., and Ryde, U. (2005) How the Co–C bond is cleaved in coenzyme B12 enzymes: a theoretical study, *J. Am. Chem. Soc. 127*, 9117–9128.

11. Sharma, P. K., Chu, Z. T., Olsson, M. H., and Warshel, A. (2007) A new paradigm for electrostatic catalysis of radical reactions in vitamin B12 enzymes, *Proc. Natl. Acad. Sci. U.S.A. 104*, 9661–9666.
12. Shibata, N., Masuda, J., Morimoto, Y., Yasuoka, N., and Toraya, T. (2002) Substrate-induced conformational change of a coenzyme B12-dependent enzyme: crystal structure of the substrate-free form of diol dehydratase, *Biochemistry 41*, 12607–12617.
13. Masuda, J., Shibata, N., Morimoto, Y., Toraya, T., and Yasuoka, N. (2000) How a protein generates a catalytic radical from coenzyme B(12): X-ray structure of a diol-dehydratase-adeninylpentylcobalamin complex, *Structure 8*, 775–788.
14. Shibata, N., Tamagaki, H., Hieda, N., Akita, K., Komori, H., Shomura, Y., Terawaki, S. I., Mori, K., Yasuoka, N., Higuchi, Y., Toraya, T. (2010) Crystal structures of ethanolamine ammonia-lyase complexed with coenzyme B12 analogs and substrates. *J. Biol. Chem.* DOI: 10.1074/jbcM110.125112.
15. Gruber, K., Reitzer, R., and Kratky, C. (2001) Radical shuttling in a protein: Ribose pseudorotation controls alkyl-radical transfer in the coenzyme B(12) dependent enzyme glutamate mutase, *Angew. Chem., Int. Ed. 40*, 3377–3380.
16. Licht, S. S., Booker, S., and Stubbe, J. (1999) Studies on the catalysis of carbon-cobalt bond homolysis by ribonucleoside triphosphate reductase: evidence for concerted carbon-cobalt bond homolysis and thiyl radical formation, *Biochemistry 38*, 1221–1233.
17. Licht, S. S., Lawrence, C. C., and Stubbe, J. (1999) Thermodynamic and kinetic studies on carbon-cobalt bond homolysis by ribonucleoside triphosphate reductase: the importance of entropy in catalysis, *Biochemistry 38*, 1234–1242.
18. Brown, K. L., and Li, J. (1998) Activation parameters for the carbon-cobalt bond homolysis of coenzyme B-12 induced by the B-12-dependent ribonucleotide reductase from *Lactobacillus leichmannii*, *J. Am. Chem. Soc. 120*, 9466–9474.
19. Chen, D., Abend, A., Stubbe, J., and Frey, P. A. (2003) Epimerization at carbon-5′ of (5′*R*)-[5′-2*H*]adenosylcobalamin by ribonucleoside triphosphate reductase: cysteine 408-independent cleavage of the Co-C5′ bond, *Biochemistry 42*, 4578–4584.
20. Sintchak, M. D., Arjara, G., Kellogg, B. A., Stubbe, J., and Drennan, C. L. (2002) The crystal structure of class II ribonucleotide reductase reveals how an allosterically regulated monomer mimics a dimer, *Nat. Struct. Biol. 9*, 293–300.
21. Gerfen, G. J., Licht, S., Willems, J. P., Hoffmann, B. M., and Stubbe, J. (1996) Electron paramagnetic resonance observations of a kinetically competent intermediate formed in ribonucleotide reduction: evidence for a thiyl radical-cob(II)alamin interaction, *J. Am. Chem. Soc. 118*, 8192–8197.
22. Jordan, A., Torrents, E., Jeanthon, C., Eliasson, R., Hellman, U., Wernstedt, C., Barbé, J., and Reichard, P. (1997) B12-dependent ribonucleotide reductases from deeply rooted eubacteria are structurally related to the aerobic enzyme from *Escherichia coli.*, *Proc. Natl. Acad. Sci. U.S.A. 94*, 13487–13492.
23. Eliasson, R., Pontis, E., Jordan, A., and Reichard, P. (1999) Allosteric control of three B_{12}-dependent (Class II) ribonucleotide reductases. Implications for the evolution of ribonucleotide reduction, *J. Biol. Chem. 274*, 7182–7189.
24. Lundin, D., Torrents, E., Poole, A. M., and Sjoberg, B. M. (2009) RNRdb, a curated database of the universal enzyme family ribonucleotide reductase, reveals a high level of misannotation in sequences deposited to Genbank, *BMC Genomics 10*, 589.
25. Larsson, K. M., Jordan, A., Eliasson, R., Reichard, P., Logan, D. T., and Nordlund, P. (2004) Structural mechanism of allosteric substrate specificity regulation in a ribonucleotide reductase, *Nat. Struct. Mol. Biol. 11*, 1142–1149.
26. Brown, K. L., Zou, X., Li, J., and Chen, G. (2001) Enzymatic activity of coenzyme B(12) derivatives with altered axial nucleotides: probing the mechanochemical triggering hypothesis in ribonucleotide reductase, *Inorg. Chem. 40*, 5942–5947.
27. Dölker, N., Maseras, F., and Siegbahn, P. E. M. (2004) Stabilization of the adenosyl radical in coenzyme B-12—a theoretical study, *Chem. Phys. Lett. 386*, 174–178.
28. Licht, S. S., Lawrence, C. C., and Stubbe, J. (1999) Class II ribonucleotide reductases catalyze carbon-cobalt bond reformation on every turnover, *J. Am. Chem. Soc. 121*, 7463–7468.
29. Uhlin, U., and Eklund, H. (1994) Structure of ribonucleotide reductase protein R1, *Nature 370*, 533–539.
30. Logan, D. T., Andersson, J., Sjöberg, B.-M., and Nordlund, P. (1999) A glycyl radical site in the crystal structure of a class III ribonucleotide reductase, *Science 283*, 1499–1504.
31. Kabsch, W. (2001) XDS, in *International Tables for Crystallography, Vol. F: Crystallography of Biological Macromolecules* (Rossmann, M. G., and Arnold, E., Eds.), Kluwer Academic Publishers, Dordrecht.
32. Otwinowski, Z. , Minor, W. (1997) Processing of X-ray diffraction data collected in oscillation mode, in *Methods in Enzymology* (Carter, C. W., Jr., and Sweet, R. M. , Eds.), pp 307–326, Academic Press, New York.
33. Collaborative Computational Project, no. 4 (1994) The CCP4 suite: programs for protein crystallography, *Acta Crystallogr., Sect. D: Biol. Crystallogr.* 50, 760–763.
34. Potterton, E., Briggs, P., Turkenburg, M., and Dodson, E. (2003) A graphical user interface to the CCP4 program suite, *Acta Crystallogr., Sect. D: Biol. Crystallogr. 59*, 1131–1137.
35. Adams, P. D., Grosse-Kunstleve, R. W., Hung, L. W., Ioerger, T. R., McCoy, A. J., Moriarty, N. W., Read, R. J., Sacchettini, J. C., Sauter, N. K., and Terwilliger, T. C. (2002) PHENIX: building new software for automated crystallographic structure determination, *Acta Crystallogr., Sect. D: Biol. Crystallogr. 58*, 1948–1954.
36. Ouyang, L., Rulis, P., Ching, W. Y., Nardin, G., and Randaccio, L. (2004) Accurate redetermination of the X-ray structure and electronic bonding in adenosylcobalamin, *Inorg. Chem. 43*, 1235–1241.
37. Jones, T. A., Zou, J. Y., Cowan, S. W., and Kjeldgaard, (1991) Improved methods for building protein models in electron density maps and the location of errors in these models, *Acta Crystallogr. A47*, (Pt 2), 110–119.
38. Emsley, P., and Cowtan, K. (2004) Coot: model-building tools for molecular graphics, *Acta Crystallogr., Sect. D: Biol. Crystallogr. 60*, 2126–2132.
39. Krissinel, E., and Henrick, K. (2004) Secondary-structure matching (SSM), a new tool for fast protein structure alignment in three dimensions, *Acta Crystallogr., Sect. D: Biol. Crystallogr. 60*, 2256–2268.
40. Davis, I. W., Leaver-Fay, A., Chen, V. B., Block, J. N., Kapral, G. J., Wang, X., Murray, L. W., Arendall, W. B., 3rd, Snoeyink, J., Richardson, J. S., and Richardson, D. C. (2007) MolProbity: all-atom contacts and structure validation for proteins and nucleic acids, *Nucleic Acids Res. 35*, W375–383.